NASA TECHNICAL MEMORANDUM 89032

ENERGY DISSIPATION ASSOCIATED WITH CRACK EXTENSION IN AN ELASTIC-PLASTIC MATERIAL

K. N. Shivakumar and J. H. Crews, Jr.

JANUARY 1987

National Aeronautics and Space Administration

Langley Research Center
Hampton, Virginia 23665

SUMMARY

Crack extension in elastic-plastic material involves energy dissipation through the creation of new crack surfaces and additional yielding around the crack front. An analytical procedure, using a two-dimensional elastic-plastic finite element method, was developed to calculate the energy dissipation components during a quasi-static crack extension. The fracture of an isotropic compact specimen was numerically simulated using the critical crack-tip-opening-displacement (CTOD) growth criterion. Two specimen sizes were analyzed for three values of critical CTOD. Results from the analyses showed that the total energy dissipation rate consisted of three components: 1) the crack separation energy rate G_s, 2) the plastic energy dissipation rate G_p, and 3) the residual strain energy rate G_{rs}. All three energy dissipation components and the total energy dissipation rate initially increased with crack extension and finally reached constant values. For ductile materials (larger CTOD), G_p becomes dominant (more than 70% of the total), whereas G_{rs} remained constant (about 6%). Furthermore, G_p appeared to vary linearly with the plastic zone height. G_s is linearly proportional to the critical CTOD.

INTRODUCTION

Crack extension in an elastic-plastic material involves energy dissipation through the creation of new crack surfaces and by yielding. An understanding of the fracture energy dissipation process may provide guidance for developing tougher materials and could also provide a basis for predicting energy absorption during failure. Several energy dissipation analyses have been performed for an extending crack.

Kfouri and Miller [1,2] performed an elastic-plastic finite element analysis of a center crack specimen. The crack was extended by a finite amount by releasing the crack-tip force. The work done by the crack-tip force and the associated displacement was defined as the crack separation energy. The crack separation energy rate was assumed to be the total energy dissipation associated with crack extension [1-3]. In these analyses the energy dissipation due to additional yielding during each increment of crack extension was neglected.

Turner [4] hypothesized that for a global energy balance the total dissipation energy is sum of the crack separation energy and the plastic energy dissipated during crack extension. He assumed that the total energy dissipation rate was the sum of the elastic strain energy release rate, calculated by assuming an elastic response, plus the plastic energy dissipation rate. This mathematical representation was based on an heuristic argument for a center crack specimen without mathematical proof.

The objective of the present study was to develop an analytical procedure to calculate the various energy dissipation components during crack extension and to relate them to the total energy dissipation computed from the global load-displacement response.

A two-dimensional, elastic-plastic, finite element analysis [5] was used to implement the procedure. A standard compact specimen made of an elastic-plastic material was analyzed. The specimen was modeled using constant strain triangular elements. Fracture was analytically simulated using the critical crack-tip-opening-displacement (CTOD) criterion. The crack was extended by releasing the force at the crack tip in steps. The analysis was repeated for three material toughnesses, which were simulated by using three different values for the critical CTOD. The magnitudes of the energy dissipation components were compared with the total energy dissipation for the different material toughnesses. The effect of critical CTOD on crack separation and plastic energy dissipation rates was also examined.

ANALYSIS

Figure 1 shows the compact tension specimen of width w and crack length a with loading P. In the analysis, a displacement was applied and then the load was calculated. The initial crack-length-to-width ratio was 0.5. The specimen was assumed to be under plane-strain conditions. The material was typical of an aluminum alloy with Young's modulus E = 71 GPa, Poisson's ratio ν = 0.3, and the 0.2% offset yield stress σ_y = 315 MPa. The

uniaxial stress-strain response of the material was represented by the Ramberg-Osgood equation $\epsilon = (\sigma/E) + (\sigma/\kappa)^n$, where $\kappa =$ 551.6 MPa and $n = 10$.

As previously mentioned, a two-dimensional, elastic-plastic finite element analysis and the critical crack-tip-opening-displacement (CTOD) criterion were used to simulate the fracture of the compact specimen [5]. Equations are presented in the following sections to calculate the energy dissipation rates associated with crack extension. Then the analytical fracture simulation is explained using the finite element analysis.

Energy Dissipation During Crack Growth

Although the procedure is general, the focus here is on the use of a finite element analysis to calculate the energy dissipation components in a compact specimen. The fracture processes in elastic and elastic-plastic specimens are discussed separately in the following sections. The viscoelastic effects of the material are neglected.

Elastic materials.- Two methods for calculating the change in elastic energy during crack growth are presented. One is based on the global load and load-point displacement. The other uses the crack-tip force and displacement. Figure 2(a) shows a typical load-displacement curve for an elastic compact specimen. The initial crack length is a. When the load reaches P_A, the crack becomes critical and grows by an element size Δa. Simultaneously, the load drops to P_B in this displacement controlled case. The total energy dissipated in the crack growth

process is the shaded area ΔE_t. The term ΔE_t can be calculated from the loads P_A and P_B, and the specimen compliances C_a and $C_{a+\Delta a}$ before and after the crack extension.

$$\Delta E_t = (P_A^2 C_a - P_B^2 C_{a+\Delta a})/2 \qquad (1)$$

Then the total energy dissipation rate G_T, which is commonly referred to as the strain energy release rate, is

$$G_T = \frac{\Delta E_t}{(\Delta a)\ b} \qquad (2)$$

The specimen thickness b is assumed to be unity.

Figure 2(b) shows a typical relationship between the crack-tip force F and the tip separation displacement δ, obtained from a finite element analysis when the crack was extended by Δa. Point A corresponds to the critical condition just before the crack growth; the crack-tip force is F_A and $\delta = 0$. When crack extends by Δa, the force drops to zero and the displacement increases linearly to δ_B. The work done by the crack-tip force and the separation displacement is referred to as the crack separation energy ΔE_s [1,2].

$$\Delta E_s = \frac{F_A\ \delta_B}{2} \qquad (3)$$

The corresponding crack separation energy rate G_s is

$$G_s = \frac{F_A\ \delta_B}{2\ \Delta a\ b} \qquad (4)$$

Because there is no other energy dissipation process for the elastic case, $G_s = G_T$.

Elastic-plastic materials.- In contrast to the elastic case, an elastic-plastic material undergoes plastic deformation at the crack tip during crack extension. The plastic deformation causes plastic energy dissipation. In addition, the plastic deformation associated with the crack extension was found to change the residual stress-strain conditions near the crack tip, which changes the residual strain energy. As a result, the total energy dissipation associated with crack extension in an elastic-plastic material consists of three parts: 1) the crack separation energy, 2) the plastic energy dissipation, and 3) the change in the residual strain energy. This total energy dissipation, based on local response, was compared to the global load-displacement response.

Figure 3(a) shows a global load-displacement curve for an elastic-plastic compact specimen. During loading, the specimen yields around the crack tip and, therefore, the curve is nonlinear. With continued loading, the crack becomes critical, for example, at load P_A. If the specimen were unloaded from point A, the load-displacement record would follow the linear path AD. (In real specimens, unloading can cause crack closure and reverse yielding, which may cause nonlinear unloading. However, for the present purpose of calculating the energy during crack extension, a linear unloading curve was assumed.) If instead of unloading to point D, the crack is extended while holding the displacement constant, the load drops to P_B. Again, unloading would be linear and represented by the line BC, which

has a different slope than the line AD. The total energy dissipated ΔE_t due to the Δa crack extension is shown as the shaded area in figure 3(a).

$$\Delta E_t = \{P_A^2 C_a - P_B^2 C_{a+\Delta a}\}/2 \tag{5}$$

The total energy dissipation rate G_T is

$$G_T = \frac{\Delta E_t}{\Delta a\ b} \tag{6}$$

In figure 3(a), the area OAD represents the plastic energy dissipated before the crack extended. This energy dissipation may influence the crack initiation but does not contribute to the energy dissipation associated with the crack extension.

The crack separation energy rate was calculated in the same way as in the elastic case. Figure 3(b) shows the crack-tip force against separation displacement curve for a crack extension of Δa. In contrast to elastic case, the force-displacement curve is nonlinear. The work done by the crack-tip force can be calculated by integrating the area under this curve. Then the crack separation energy rate G_s is

$$G_s = \frac{1}{\Delta a\ b} \int_0^{\delta} F\ d\delta \tag{7}$$

The crack-tip force F is limited for an elastic-plastic material by the material yielding, but is unrestricted if the material is assumed to be elastic. Hence, the separation energy rate G_s for an elastic-plastic material can be much smaller than that for an assumed elastic.

The plastic energy dissipation was calculated for each finite element by integrating its plastic strain over the complete load history. Figure 3(c) shows the typical stress-strain response in an element. The stress-strain states before and after the crack growth are represented by points A and B, respectively. The shaded area above the abscissa represents the plastic energy dissipation during crack growth. The summation of such areas for all elements gives the total plastic energy dissipation ΔE_p. The term ΔE_p can be calculated from the plastic strains ϵ_p as follows:

$$\Delta E_p = \int_v \int_{\epsilon_p^A}^{\epsilon_p^B} \sigma \, d\epsilon_p \, dv \tag{8}$$

Here ϵ_p is the plastic strain and the superscripts A and B represent the conditions before and after the crack extension. Note that the plastic dissipation energy always increases, even with a load drop during crack growth. The corresponding plastic energy dissipation rate G_p is

$$G_p = \frac{\Delta E_p}{\Delta a \; b} \tag{9}$$

Residual stresses are created by the plastic deformation near the crack tip. In the present analysis, residual stresses were calculated by unloading the specimen before and after each increment of crack extension. As previously mentioned, such unloading could cause crack closure and reverse compression yielding. However, for the purpose of calculating the residual

strain energy, the crack surfaces were allowed to pass one another during unloading and the material was assumed to be elastic during unloading. Figure 3(c) shows the residual strain energies (shaded areas below abscissa) before and after the crack growth. The difference in these two areas were summed for all elements to calculate the change in the residual strain energy ΔE_{rs} during an increment of crack growth.

$$\Delta E_{rs} = \int_{v} [\frac{3}{2} \frac{(1-2\nu)}{E} (\sigma^2_{m_D} - \sigma^2_{m_C}) + \frac{(1+\nu)}{3E} (\sigma^2_{e_D} - \sigma^2_{e_C})] dv \qquad (10)$$

where σ_m and σ_e represent the mean (hydrostatic component) and the effective (deviatoric component) residual stresses, respectively. Subscripts D and C represent the unloaded conditions before and after crack growth. The residual strain energy rate G_{rs} is

$$G_{rs} = \frac{\Delta E_{rs}}{\Delta a\ b} \qquad (11)$$

Although the presence of residual stresses has been widely recognized and studied, this is believed to be the first analysis that shows their contribution to the total energy dissipation rate (G_T) for crack extension.

The G_s (Eqn. 7), G_p (Eqn. 9), and G_{rs} (Eqn. 11) terms can be summed to represent G_T calculated using the local response near the crack tip. Comparison of this local G_T with the global G_T (Eqn. 6) provided an evaluation of the analysis.

Finite Element Simulation of Crack Extension

A two-dimensional, elastic-plastic finite element analysis [5], developed at NASA Langley, was used in this study. The analysis uses constant strain triangular elements, the small strain assumption, and the von Mises yield criterion. The details of the analysis are given in [5]. The computer program was modified to include the calculation of the energy dissipation components at each increment of load and crack extension. The energy dissipation rates G_T, G_s, G_p, and G_{rs} were calculated from equations 6, 7, 9, and 11, respectively.

Figure 4 shows a finite element idealization of a 50 mm wide specimen. Since the problem shown in figure 1 is symmetric, only the top half of the specimen was modeled. The region along the crack line was finely idealized and the same mesh refinement was used over the complete uncracked width of the specimen. Such an idealization maintains a constant mesh refinement around the crack tip as the crack extends. The smallest element size was 0.4 mm, which was also the crack extension increment. The model had 2688 elements and 1462 nodes. The specimen was loaded by specifying the y-displacement at the loading point. A displacement-controlled analysis was used to provide results (load and crack extension) beyond the maximum load. As the load was increased, the specimen yielded at the crack tip. Beyond this initial yielding, the specimen was loaded incrementally as a percentage of the initial yield load. The continued loading

blunts and then opens the crack tip. At each load increment, the opening displacement at the first node behind the crack tip was monitored. When it reached or exceeded the preselected critical crack opening displacement (δ_c), the crack tip was extended by releasing the crack-tip force in several steps. (Three steps were used for δ_c = 0.025 mm and five steps were used for δ_c = 0.040 and 0.050 mm.) Since only half the specimen was modeled, a critical CTOD of $\delta_c/2$ was used in the analysis. At each load increment and at each step of crack-tip force release, the stresses, strains, and the specimen compliance were calculated. Then the energy dissipation components G_s, G_p, G_{rs}, and G_T were calculated using equations 7, 9, 11, and 6, respectively.

The analysis was first performed for a 50 mm wide specimen using a critical CTOD δ_c = 0.025 mm measured 0.4 mm behind the crack tip. (The value of CTOD was taken from reference 5 for the an aluminum alloy.) CTOD's of 0.040 and 0.050 mm were used to simulate higher toughness materials. However, at these higher values of CTOD, the 50 mm wide specimen developed back edge yielding; hence, a 100 mm wide specimen was used. To keep the same mesh refinement pattern and crack-tip element size (0.4 mm), the mesh shown in figure 4 was scaled up by 2. Then each triangular element was subdivided into four elements by joining the mid-points of the sides. This resulted in 10,752 elements and 5,612 nodes for the 100 mm model. The value of δ_c = 0.025 mm was used with w = 50 mm and 100 mm to examine the specimen size

effect. Results obtained from the analyses are discussed in the next section.

RESULTS AND DISCUSSION

The three components of energy dissipation rate were calculated at each increment of crack extension and compared with the total energy dissipation rate (G_T). As previously mentioned, the energy dissipation was examined for three different values of critical CTOD (material toughness). Also, the active plastic zones (the region currently on the von Mises yield surface) are presented for various amounts of crack extension and for different values of CTOD.

Energy Dissipation Components

Figure 5 shows the numerically simulated load crack extension plot for the 50 mm wide compact specimen. The critical CTOD (δ_c) was 0.025 mm, which is typical of a low toughness aluminum [5]. The symbols represent the load when this CTOD criterion was satisfied. Calculations were made for a sequence of crack growth increments, each corresponding to one element size (0.4 mm). The crack was extended in steps while holding the applied displacement constant, which resulted in a load drop. The specimen was loaded again (by incrementing the displacement) until the new crack tip became critical, and the analysis was continued. After three increments of crack growth (1.2 mm), the load reached a maximum (solid symbol) and then decreased with subsequent crack extension. The analysis was stopped after about 6 mm of crack extension.

The total energy dissipation rate G_T, calculated from equation (6) at each critical load, is shown in figure 6. The G_T values increased with crack extension and reached a plateau after about 2.4 mm (or 6 increments) of crack extension. This implies that the specimen had reached the material's maximum fracture resistance.

Figure 7 shows curves for the three energy dissipation components: 1) the crack separation energy rate G_s, 2) the plastic dissipation energy rate G_p, and 3) the residual strain energy rate G_{rs}. Again, the symbols represent the calculated points. The solid symbols represent the maximum load condition. The total energy dissipation rate G_T curve from figure 6 is also shown for comparison. Like the G_T curve, all three energy dissipation components reach a plateau after an initial increase. For this low toughness material, the crack separation energy rate G_s is larger than G_p at all values of crack extension. The sum of G_s, G_p, and G_{rs} agreed with G_T, within about one percent. The stabilized value of the G_{rs} component is about 6 percent of G_T. Even though G_{rs} is relatively small, it is required to satisfy the energy balance equation, $G_T = G_s + G_p + G_{rs}$. It is widely recognized that residual stresses develop around a crack tip, but a quantification of their effects on the crack growth resistance has not been previously made.

Figure 8 shows the active plastic zones at the critical condition for the initial crack length and after several increments of crack extension. The active plastic zone is the

region enclosing the elements whose stresses currently satisfy the yield criterion. Figure 8(a) indicates the load-crack extension increments for which these active plastic zones were calculated. Figure 8(b) shows the plastic zone computed immediately before the first increment of crack extension. Even though the regions behind the crack tip in figures 8(c) through 8(f) were yielded previously, they unloaded elastically as the crack grew. Hence, the stresses in these elements do not satisfy the yield criterion. Figure(8) shows that the plastic zone size increased with crack extension and stabilized soon after the maximum load was reached. The plastic zone stabilized at 2 mm(5 increments) of crack extension. Beyond this, the active plastic zone simply translated as the crack extended. The narrow strip of yielding along the x-axis of the specimen was due to the development of high x-directional stresses in the plastic wake region. The stabilization of the plastic zone indirectly implies the constancy of energy dissipation rate, which was already shown in figure 7, and the invariance of the strain state ahead of the current crack tip. The normal strain ϵ_y and the effective strain distribution ahead of the current crack tip were examined at various amounts of crack extension and after 5 increments (2 mm) of crack extension, both strain distributions remained unchanged.

Effect of Material Toughness

The results presented in the previous section were for a 50 mm wide specimen with one value of δ_c (0.025 mm). This specimen

was found to be too small to simulate the fracture of tougher materials (higher values of δ_c) because of back edge compression yielding. Therefore, a larger size specimen, 100 mm wide, was analyzed for three different values of δ_c (0.025, 0.040, and 0.050 mm). As previously mentioned, these values of δ_c represent low, medium, and high toughnesses, typical of an aluminum alloy.

Figure 9 shows curves for the load and crack extension for the 100 mm specimen. For δ_c = 0.025 mm, the results for the 50 mm specimen are also shown. The shapes of 100 mm and 50 mm specimen curves are very similar. Both specimens reached maximum loads at 1.2 mm of crack extension. The maximum loads for δ_c = 0.040 and 0.050 mm were reached at 3.2 mm and 4.4 mm of crack extension, respectively. Therefore, the amount of crack extension required to reach the maximum load increased with material toughness.

Figure 10 shows the total energy dissipation rate G_T versus crack extension for the three values of δ_c. The G_T values were calculated from the specimen global loads and load-point displacements (equation 6). The G_T curves for the 50 and 100 mm specimens with δ_c = 0.025 mm agree very well. This shows that, for a given value of δ_c, the specimen size had no effect on the G_T resistance curve. Comparing the G_T curves for the 100 mm specimens shows that G_T increases with material toughness (δ_c). All calculated values of G_T were checked with

the respective sums of G_s, G_p, and G_{rs} and were found to agree very well.

Figure 11 shows the energy dissipation rate components normalized by G_T plotted versus the critical CTOD (δ_c). The crack separation energy ratio (G_s/G_T) decreased from 0.57 to 0.23 and the plastic energy dissipation ratio (G_p/G_T) increased from 0.37 to 0.71 when δ_c was increased from 0.025 to 0.050 mm. For larger values of δ_c (i.e., for higher toughness materials), G_s/G_T could be lower than 0.2 and G_p/G_T could be higher than 0.7. The G_{rs}/G_T ratio remained almost constant, at about .06, for the range of δ_c studied.

Figure 12(a) shows the crack-tip force and the separation displacement curves for the three values of δ_c. These curves correspond to the plateau portion of the G_s versus crack-extension curve. As previously explained, the area under the crack-tip force and displacement curve normalized by the new crack surface area Δa (the specimen thickness was unity) represents the separation energy rate G_s. For the three values of critical CTOD selected, there is a small difference in the maximum force F (at $\delta = 0$) and a large difference in the maximum opening displacements (i.e., at $F = 0$). The small difference in the maximum F was due to the material strain hardening assumed in the analysis. If the material had been elastic-perfectly plastic, the maximum F would have been identical for all three CTOD's. Therefore, the effect of material toughness on G_s was governed more by the crack-tip-opening-displacement than by the

crack-tip force. Figure 12(b) shows the plot of G_s against δ_c. The straight-line fit between G_s and δ_c suggests that G_s varies linearly with the critical crack-tip-opening-displacement (δ_c). This type of relationship was reported by Sorensen [7]. Note that while comparing results for different materials having different yield stresses, the G_s-δ_c curve need not be linear. However, G_s normalized by the yield stress could still vary linearly with δ_c.

Figure 13 shows the stabilized plastic zones for δ_c = 0.025, 0.040, and 0.050 mm. The plastic zone size increased dramatically with δ_c, which illustrates the extensive plastic deformation that accompanies crack growth in tough materials. The plastic zone size (area) for δ_c = 0.050 mm is an order of magnitude (36 times) larger than that for δ_c = 0.025 mm, even though the ratio of δ_c is only 2.

The heights (h_p) of the plastic zones shown in the figure 13 are plotted against their respective plastic energy dissipation rates G_p in figure 14. The three points shown in the figure are nearly on a straight line. The plastic energy dissipation rate varies nearly linearly with the height of the stabilized plastic zone. Once the plastic zone stabilized, the plastic zone simply translated during crack extension without changing size. The volume of "new" material yielded by the translation was proportional to h_p. Therefore, G_p should vary linearly with the plastic zone height rather than with the plastic zone area.

CONCLUDING REMARKS

A procedure was developed to calculate the components of the energy dissipation during crack extension in an elastic-plastic material. The procedure was implemented in a two-dimensional, elastic-plastic finite element program. The fracture of a compact specimen was simulated numerically using a critical crack-tip-opening-displacement (CTOD) criterion for crack growth. Two specimen sizes, 50 mm and 100 mm, were analyzed for various values of critical CTOD. The critical CTOD was varied to simulate three different material toughnesses. The total dissipation energy, its components, and the active plastic zones were examined for a range of fracture toughnesses. Based on this study the following conclusions were made:

1. The total energy dissipation rate G_T consisted of three components: the crack separation energy rate G_s, the plastic energy dissipation rate G_p, and the residual strain energy rate G_{rs}.

2. All three energy dissipation components and the total energy dissipation rate initially increased with crack extension and then reached a plateau soon after the maximum load was reached.

3. The crack separation energy rate G_s varied nearly linearly with the critical CTOD. For tougher materials, the G_s component dropped to about 20% of G_T; the G_p component became more than 70% of G_T. The plastic energy dissipation rate was

found to vary nearly linearly with the height of the plastic zone.

4. The residual strain energy rate G_{rs} was almost constant as the crack extended and was only about 6% of the total energy dissipation rate for all three toughness levels.

REFERENCES

1. Kfouri, A. P., and Miller, K. J., International Journal of Pressure Vessel and Piping, vol. 2, 1974, p. 179.

2. Kfouri, A. P., and Miller, K. J., "Crack Separation Energy Rates in Elastic-Plastic Fracture Mechanics," in Proc. Institute of Mechanical Engineering, vol. 190, No. 43, London, 1976, p. 57.

3. Kfouri, A. P. and Rice, J. R., "Elastic/Plastic Separation Energy Rate for Crack Advance in Finite Growth Steps." Fracture, 1977, vol. 1, ICF4, Waterloo, Canada, June 19-24, 1977.

4. Turner, C. E., "Description of Stable and Unstable Crack Growth in the Elastic Plastic Region in Terms of J_R Resistance Curves," Fracture Mechanics, ASTM STP 677, C. W. Smith ed., "American Society for Testing and Materials," 1979, pp. 614-628.

5. Newman, J. C., Jr., "An Elastic-Plastic Finite Element Analysis of Crack Initiation, Stable Crack Growth, and Instability." Fracture Mechanics: Fifteenth Symposium, ASTM STP 833, R. J. Sanford, Ed., American Society for Testing and Materials, 1984, pp. 93-117.

6. Zienkiewicz, O. C., Valliappan, S., and King, I. P., "Elasto-Plastic Solutions of Engineering Problems, Initial Stress, Finite Element Approach," International Journal for Numerical Methods in Engineering, vol. 1, 1969,pp. 75-100.

7. Sorensen, E. P., "A Numerical Investigation of Plane-Strain Stable Crack Growth Under Small Scale Yielding Conditions," Elastic-Plastic Fracture ASTM STP 668, J. D. Landes, J. A. Begley, and G. A. Clarke, eds., American Society for Testing and Materials, 1979, pp. 151-174.

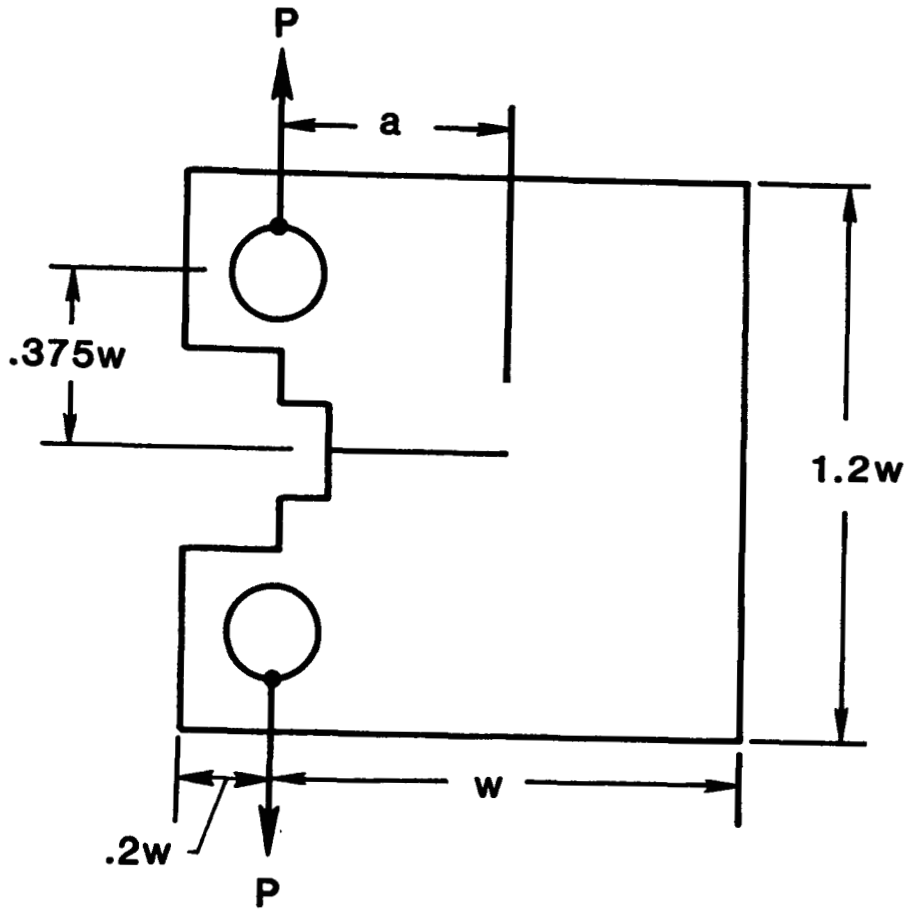

Figure 1. - Compact tension specimen and loading.

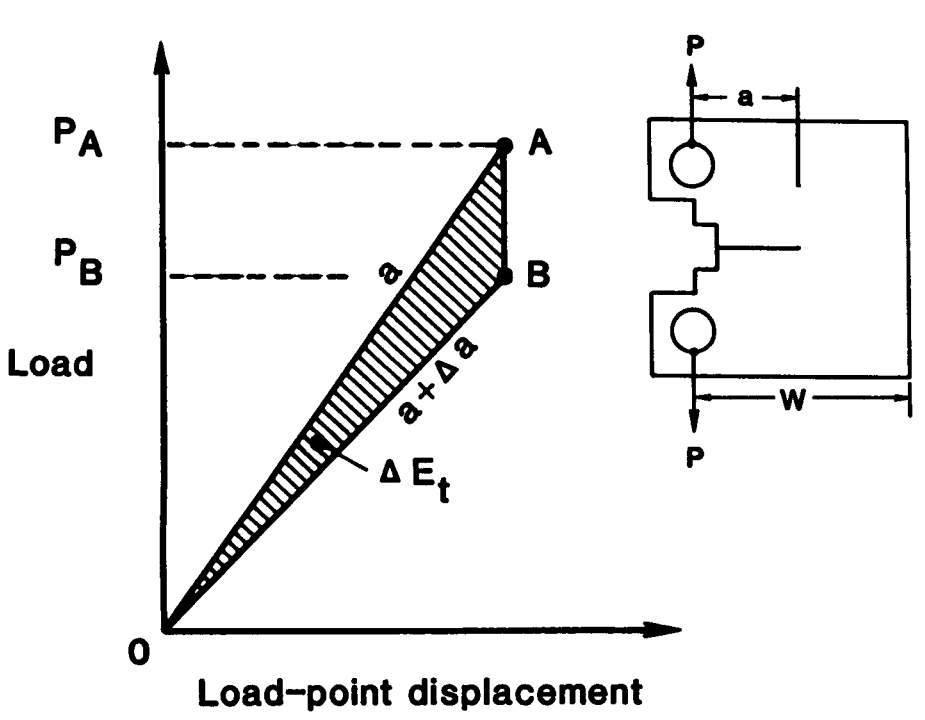

(a) Global load-displacement curve

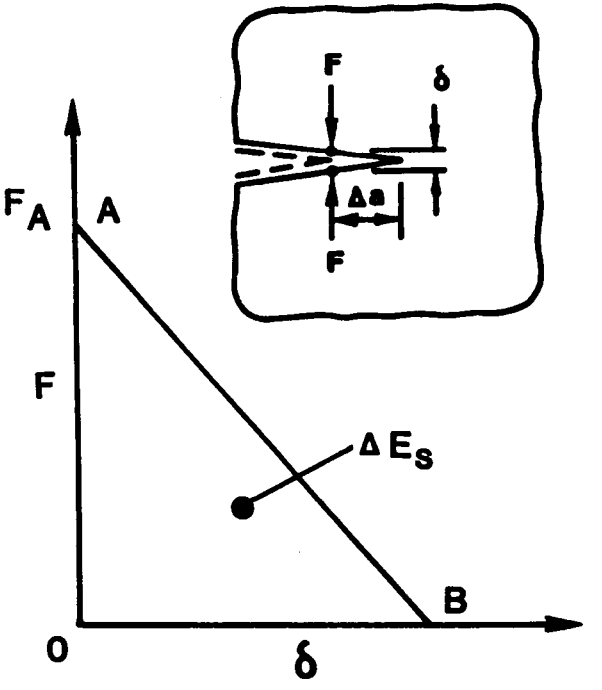

(b) Crack-tip force-displacement curve

Figure 2. - Crack extension in elastic materials.

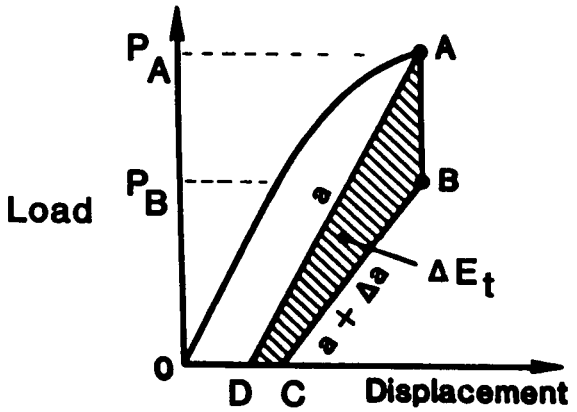

(a) Global Load–Displacement Curve

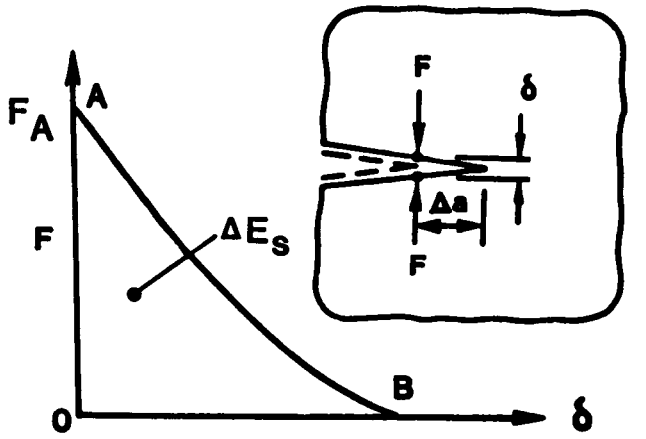

(b) Crack–Tip Force–Displacement Curve

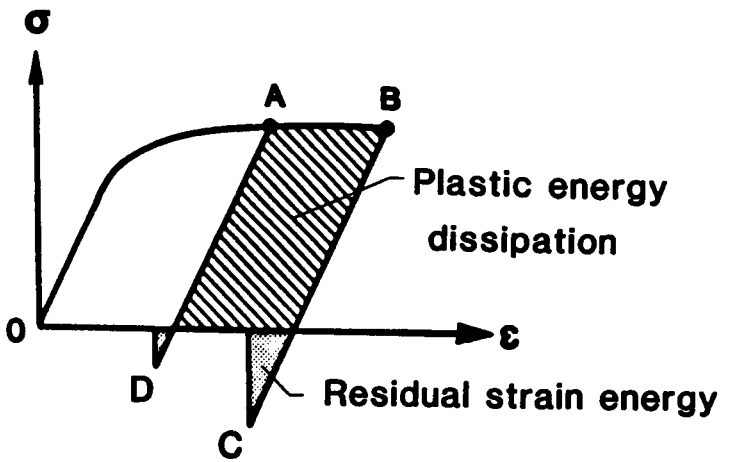

(c) Element stress-strain history

Figure 3. - Crack extension in elastic-plastic materials.

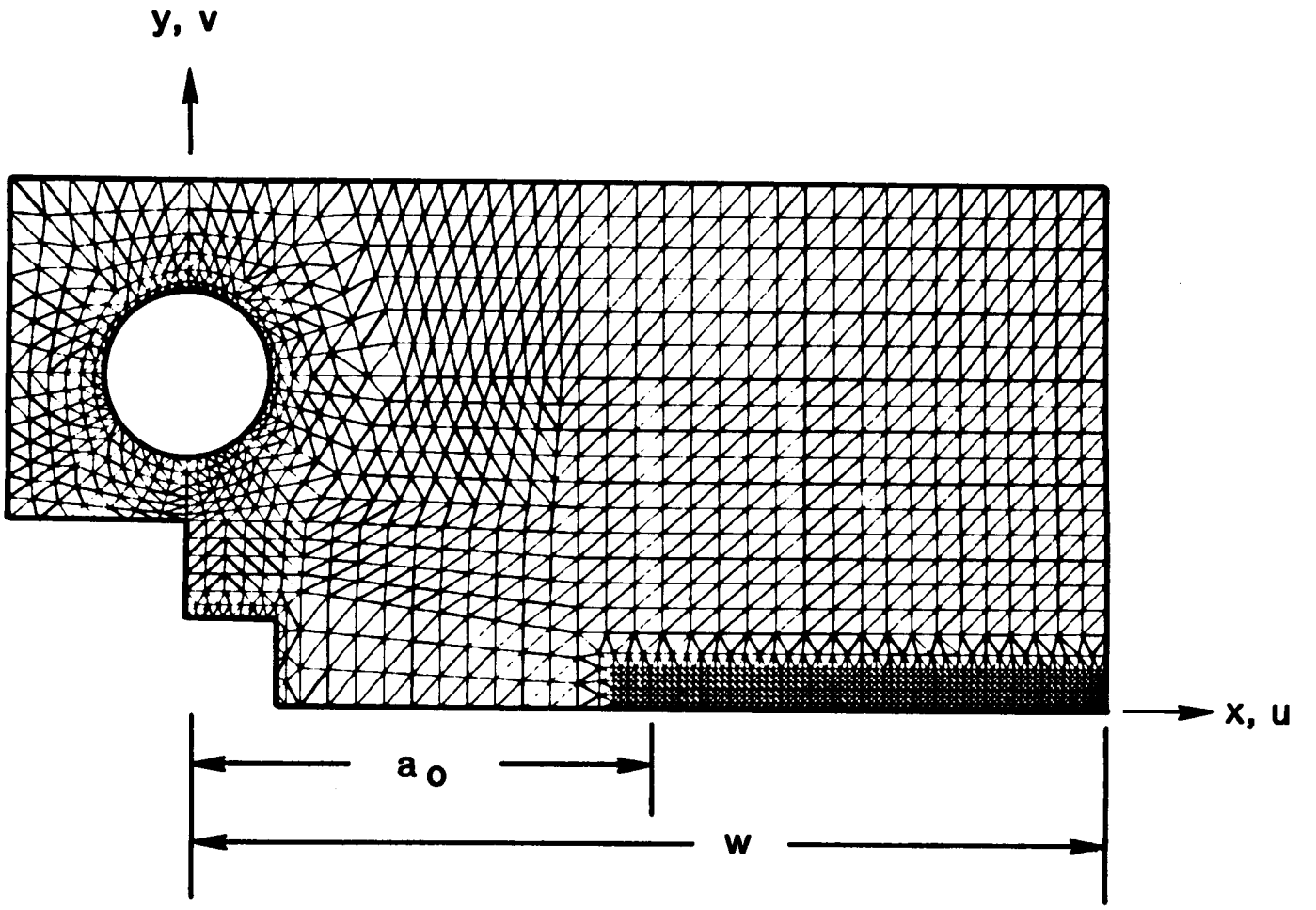

Figure 4. - Finite-element idealization for a w = 50 mm compact specimen.

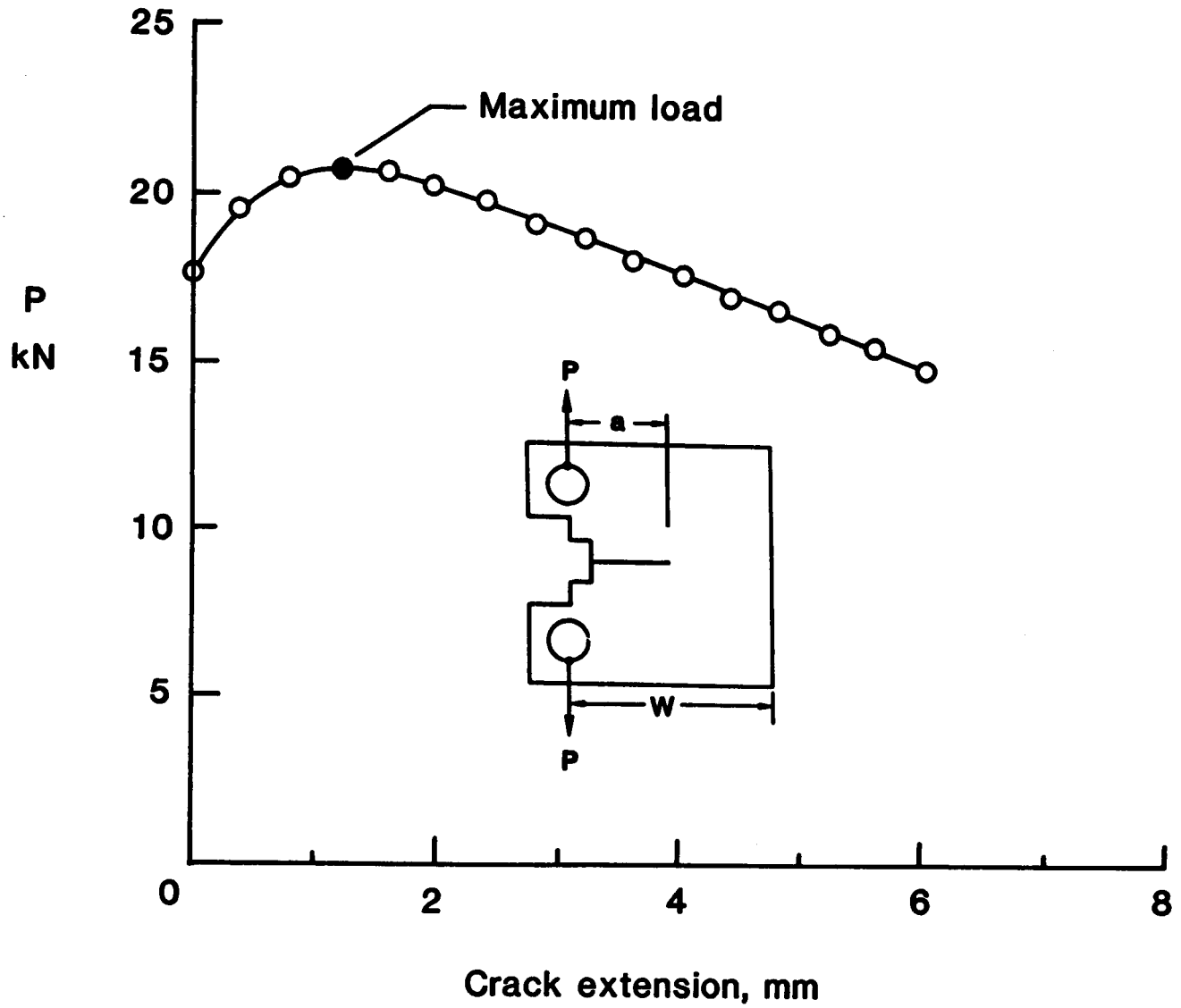

Figure 5. - Numerical simulation of load-crack extension for 50 mm wide specimen at critical CTOD = .025 mm.

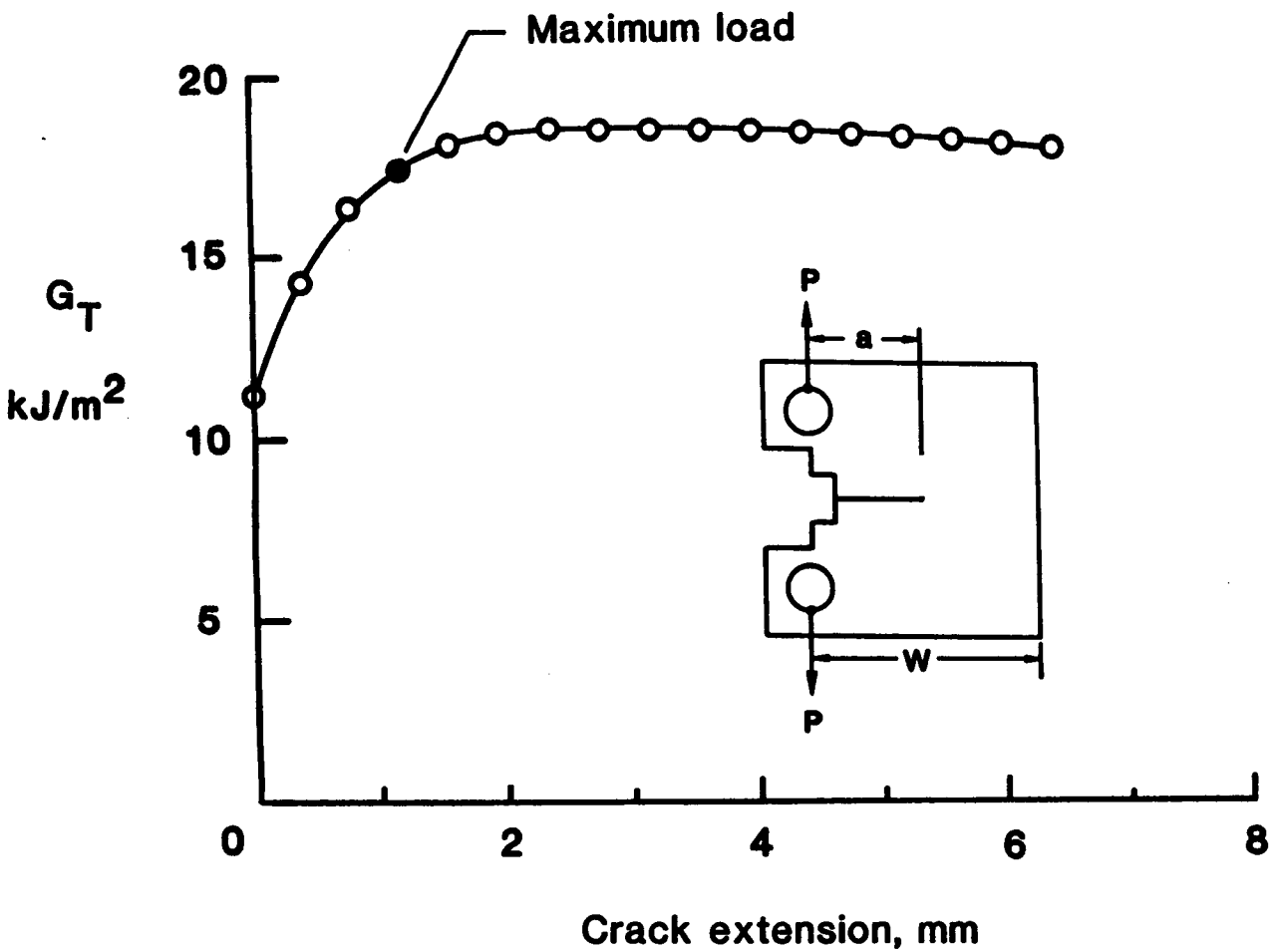

Figure 6. - Total energy dissipation rate versus crack-extension (w = 50 mm, critical CTOD = .025 mm).

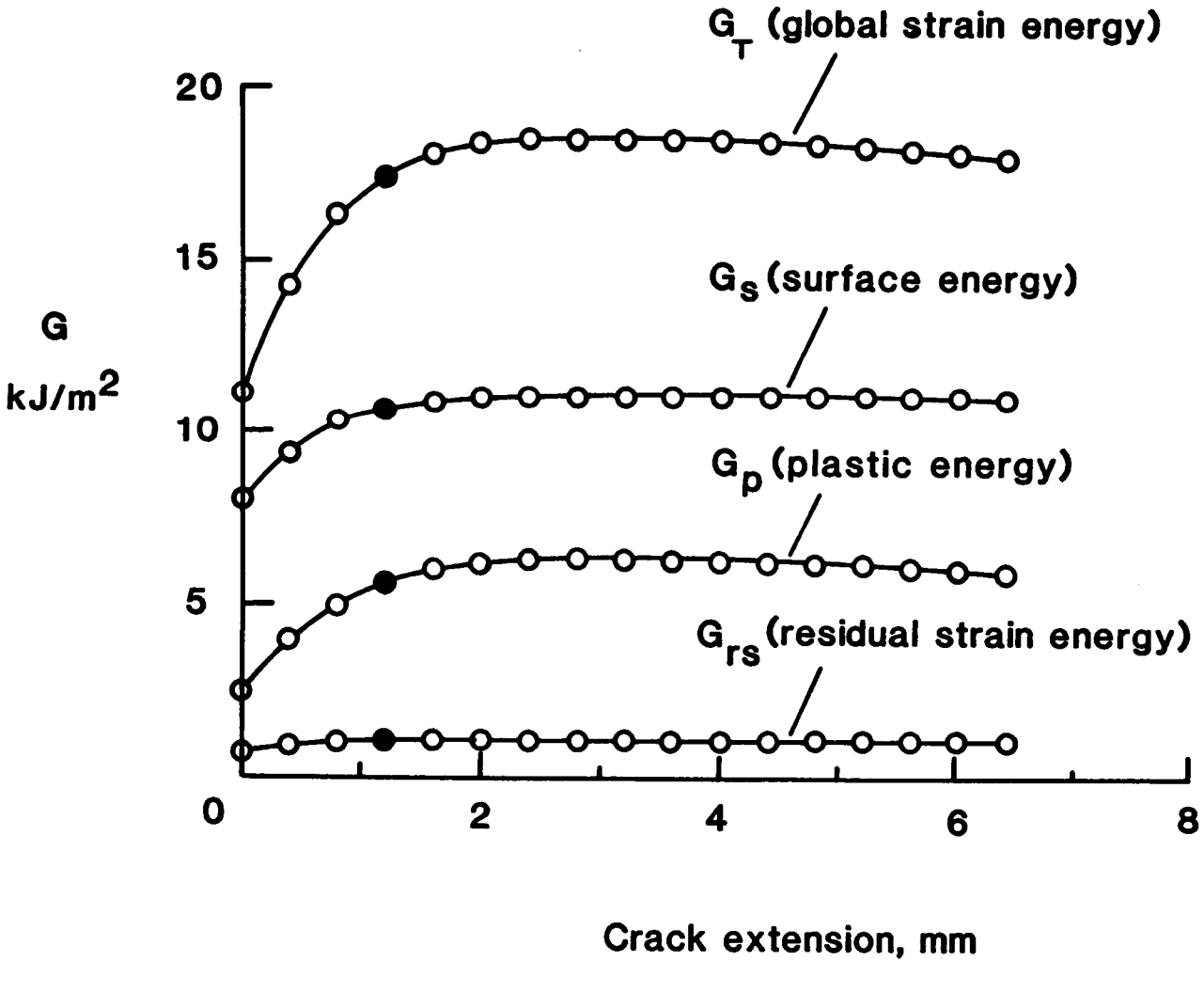

Figure 7. - Variation of energy dissipation components with crack extension (w = 50 mm, critical CTOD = .025 mm).

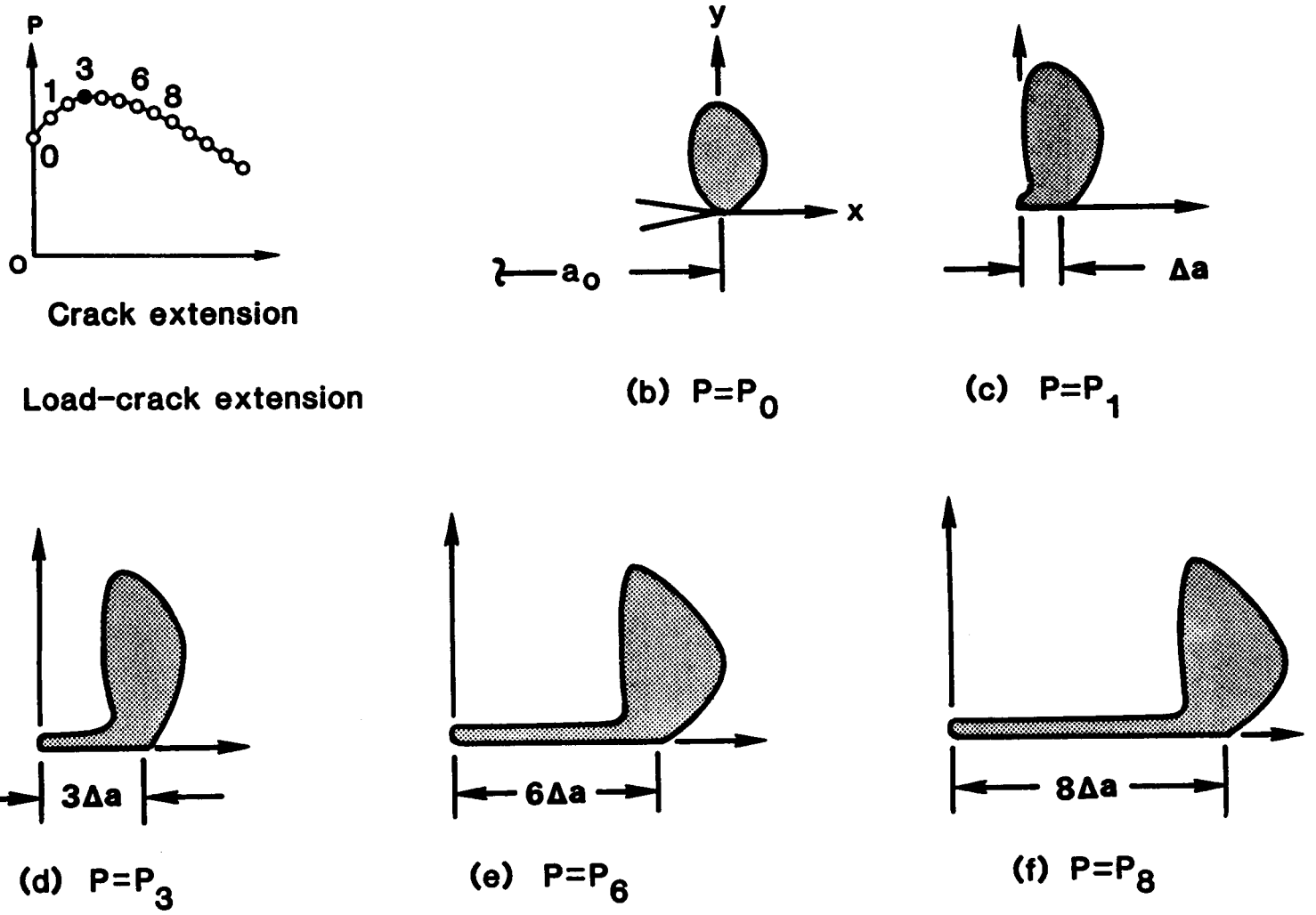

Figure 8. - Propagation of active plastic zone with crack extension (w = 50 mm, critical CTOD = .025 mm).

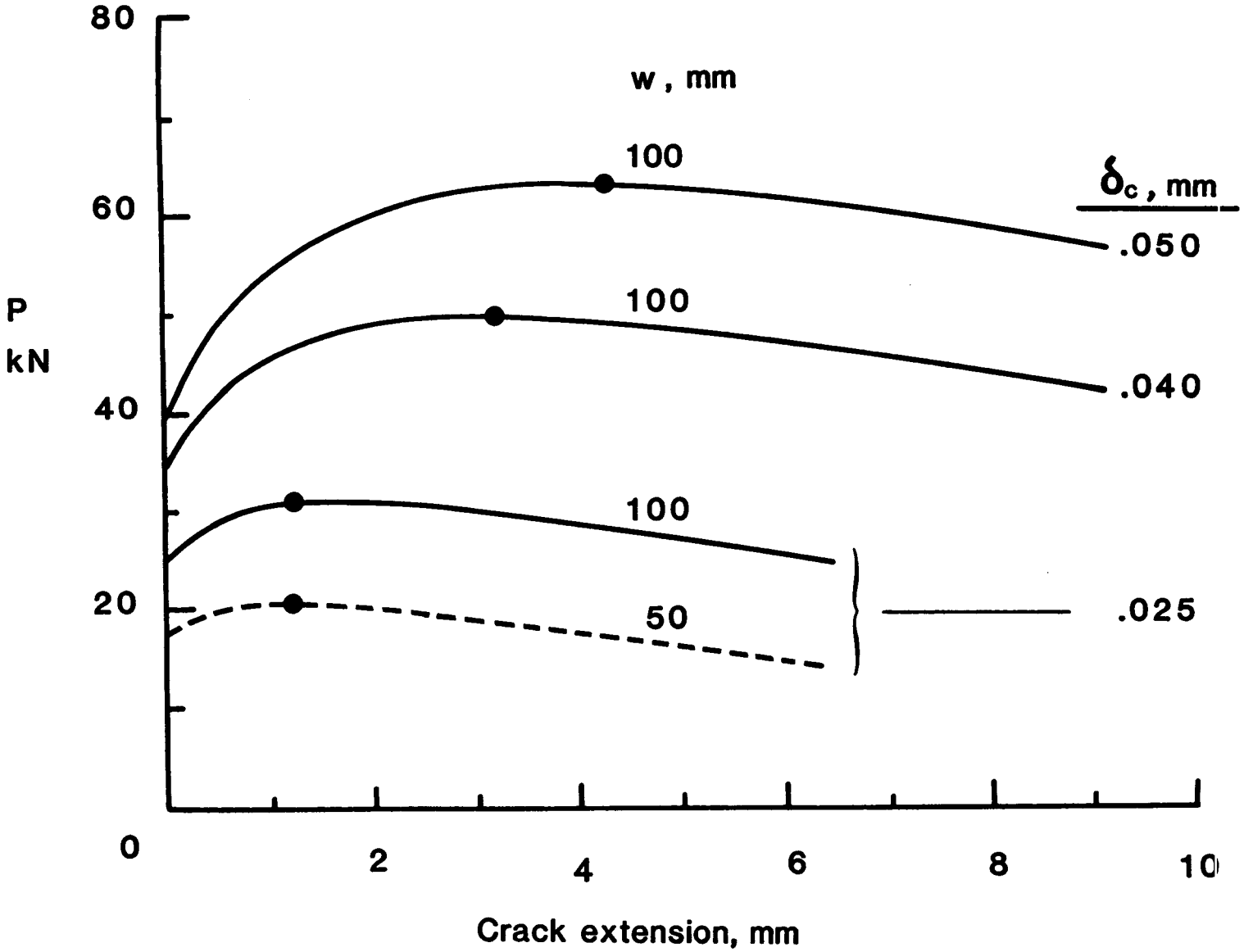

Figure 9. - Load versus crack extension for different critical CTOD and specimen width.

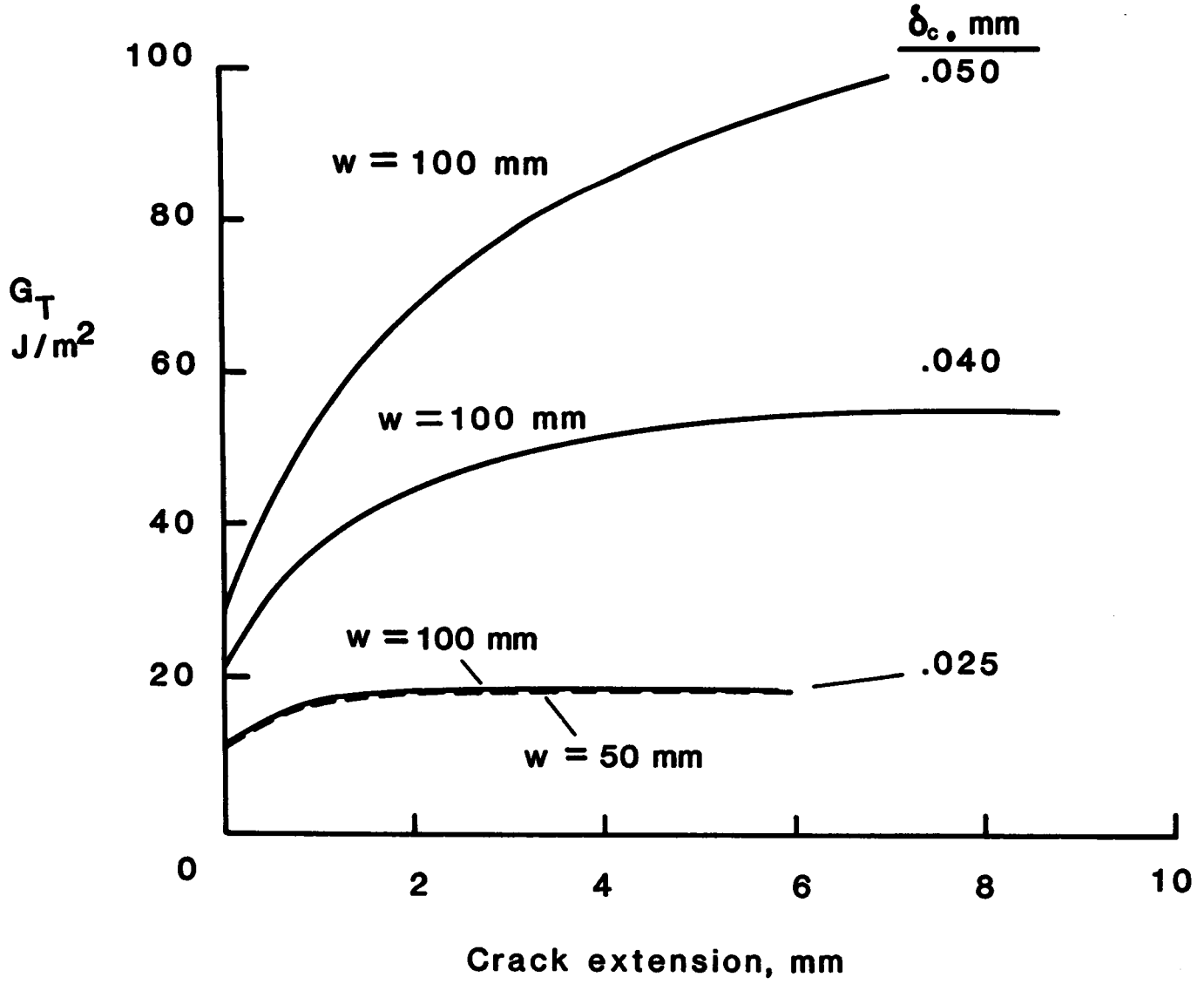

Figure 10. - Total energy dissipation rate against crack extension for different critical CTOD and specimen width.

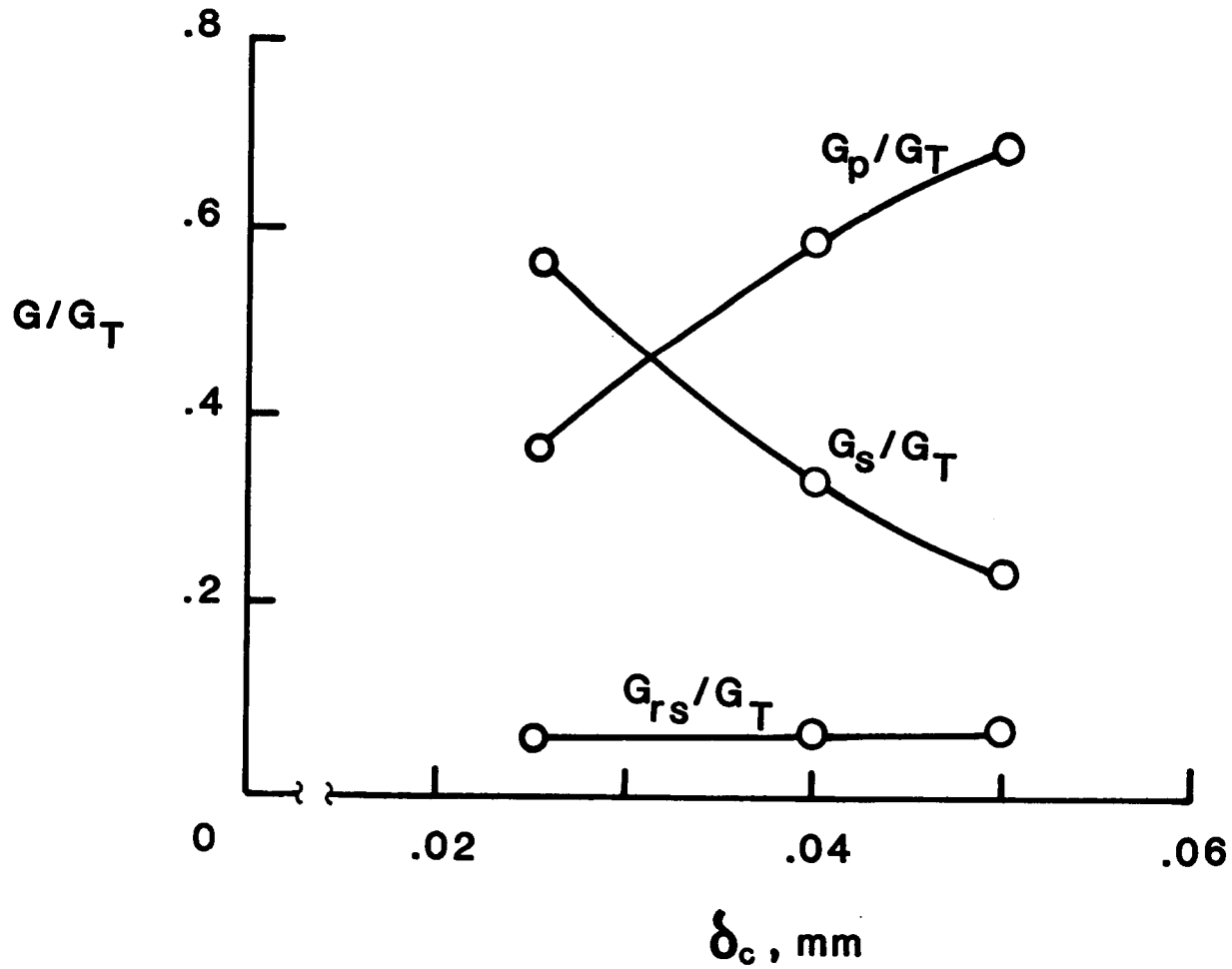

Figure 11. - Variation of normalized energy dissipation components with critical CTOD.

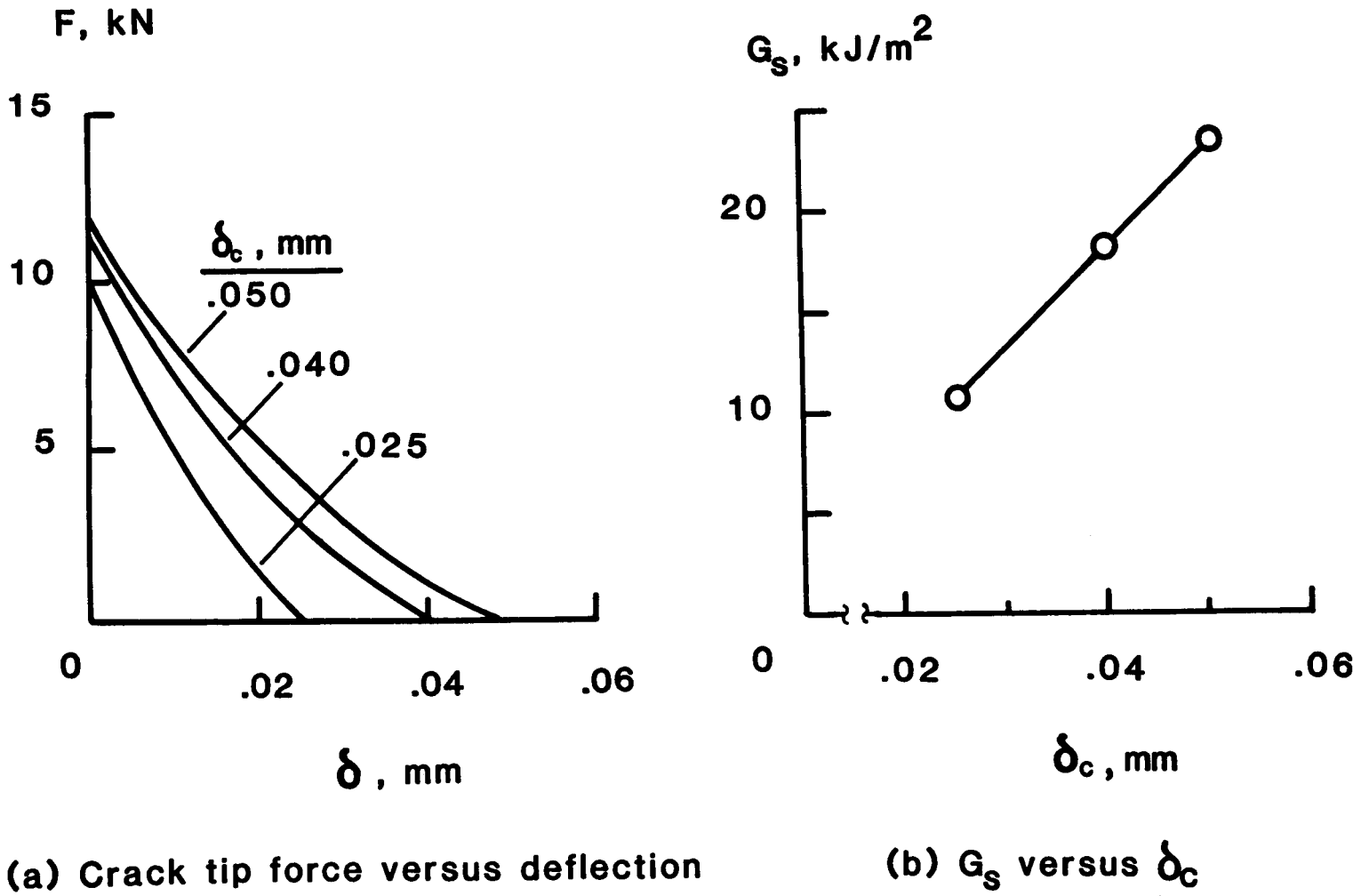

Figure 12. - Variation of crack separation energy rate G_s with critical CTOD.

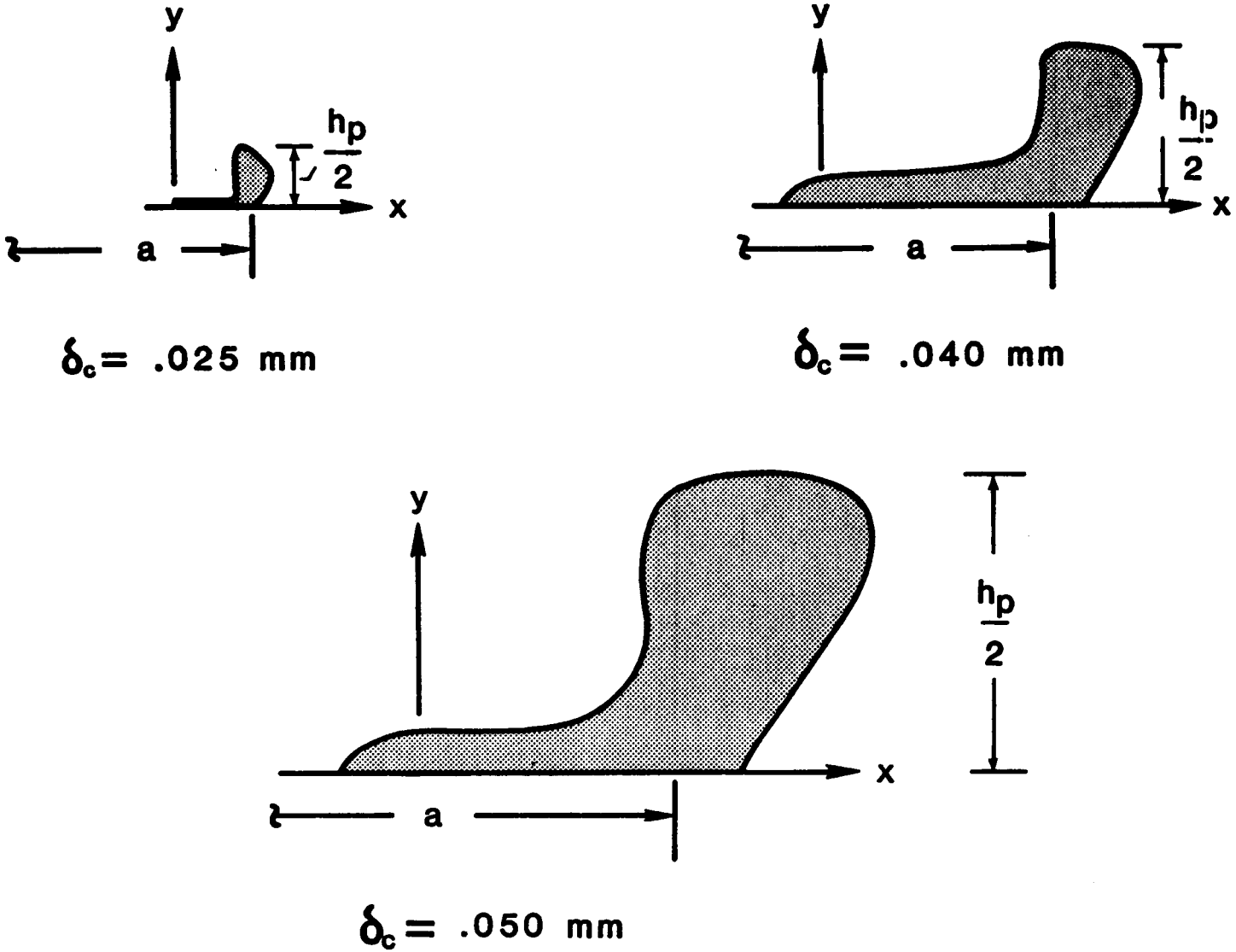

Figure 13. - Stabilized active plastic zones for different values of critical CTOD.

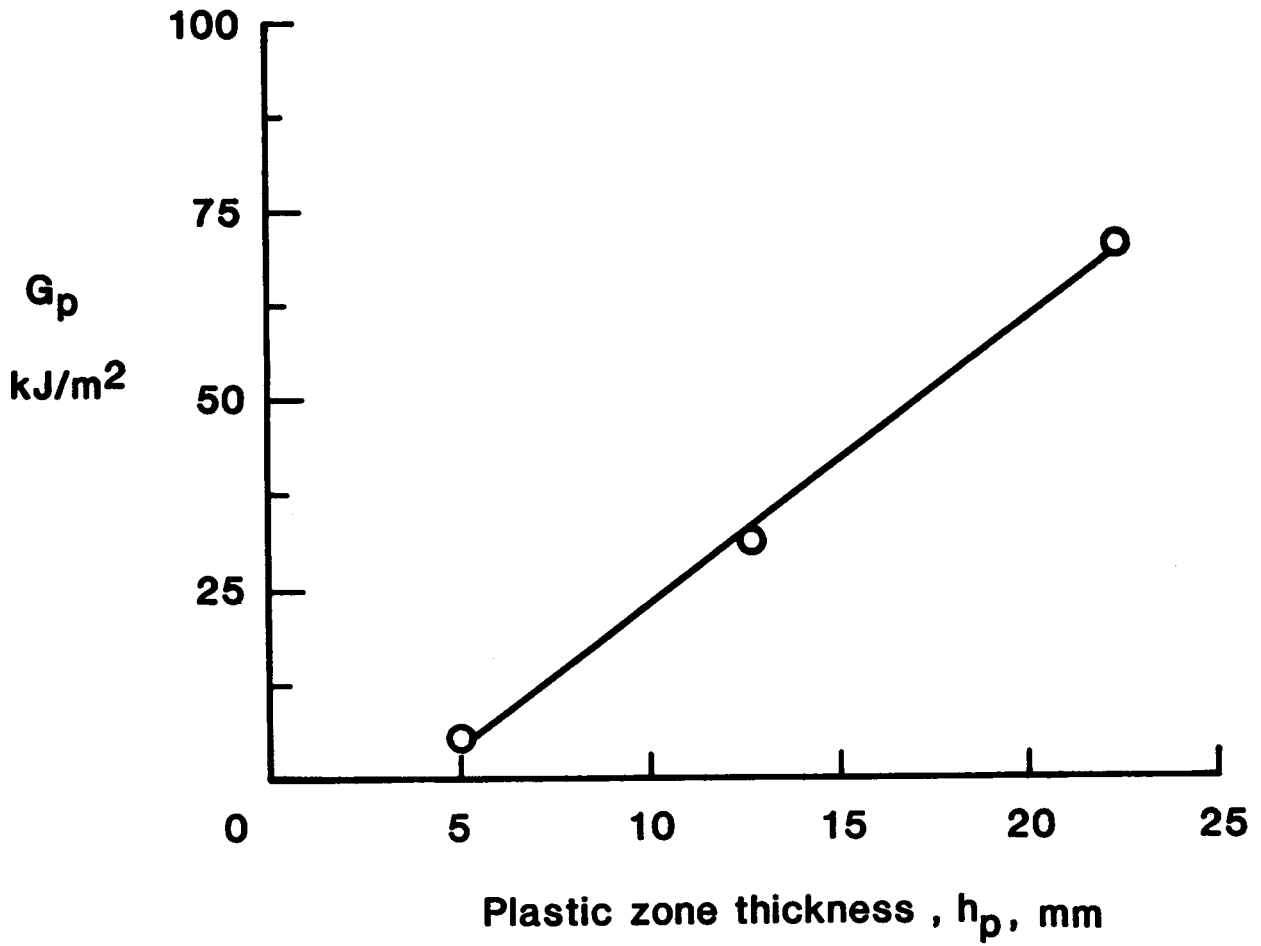

Figure 14. - Variation of stabilized plastic energy dissipation rate (G_p) with the stabilized plastic zone height (h_p).

Standard Bibliographic Page

1. Report No.	2. Government Accession No.	3. Recipient's Catalog No.
NASA TM-89032		

4. Title and Subtitle	5. Report Date
Energy Dissipation Associated with Crack Extension in an Elastic-Plastic Material	January 1987
	6. Performing Organization Code: 506-43-11-04
7. Author(s): K. N. Shivakumar* and J. H. Crews, Jr.	8. Performing Organization Report No.
9. Performing Organization Name and Address: NASA Langley Research Center, Hampton, VA 23665-5225	10. Work Unit No.
	11. Contract or Grant No.
12. Sponsoring Agency Name and Address: National Aeronautics and Space Administration, Washington, DC 20546	13. Type of Report and Period Covered: Technical Memorandum
	14. Sponsoring Agency Code

15. Supplementary Notes

*K. N. Shivakumar, Analytical Services & Materials, Inc.

16. Abstract

Crack extension in elastic-plastic material involves energy dissipation through the creation of new crack surfaces and additional yielding around the crack front. An analytical procedure, using a two-dimensional elastic-plastic finite element method, was developed to calculate the energy dissipation components during a quasi-static crack extension. The fracture of an isotropic compact specimen was numerically simulated using the critical crack-tip-opening-displacement (CTOD) growth criterion. Two specimen sizes were analyzed for three values of critical CTOD. Results from the analyses showed that the total energy dissipation rate consisted of three components: (1) the crack separation energy rate G_s, (2) the plastic energy dissipation rate G_p, and (3) the residual strain energy rate G_{rs}. All three energy dissipation components and the total energy dissipation rate initially increased with crack extension and finally reached constant values. For ductile materials (larger CTOD), G_p becomes dominant (more than 70% of the total), whereas G_{rs} remained constant (about 6%). Furthermore, G_p appeared to vary linearly with the plastic zone height. G_s is linearly proportional to the critical CTOD.

17. Key Words (Suggested by Authors(s))	18. Distribution Statement
CTOD Finite element analysis Elastic-plastic fracture Energy release rate Crack growth energy	Unclassified - Unlimited Subject Category 39

19. Security Classif.(of this report)	20. Security Classif.(of this page)	21. No. of Pages	22. Price
Unclassified	Unclassified	35	A03

For sale by the National Technical Information Service, Springfield, Virginia 22161